Supplementary data

In Vivo Visualization of Osteoarthritic Hypertrophic Lesions

Hai-Yu Hu[1,2,5], Ngee-Han Lim[3], Hans-Paul Juretschke[2], Danping Ding-Pfennigdorff[2], Peter Florian[2], Markus Kohlmann[2], Abdulah Kandira[2], Jens Peter von Kries[4], Joachim Saas[2], Karl A. Rudolphi[2], K. Ulrich Wendt[2], Hideaki Nagase[3], Oliver Plettenburg[2], Marc Nazare[2,4*], Carsten Schultz[1 *]

[1]European Molecular Biology Laboratory (EMBL), Interdisciplinary Chemistry Group, Cell Biology and Biophysics Unit, Meyerhofstr. 1, 69117 Heidelberg, Germany

[2]Sanofi-Aventis Deutschland GmbH, Industriepark Höchst, 65962 Frankfurt, Germany

[3]Kennedy Institute of Rheumatology, University of Oxford, Roosevelt Drive, Headington, Oxford OX3 7FY, United Kingdom

[4]Leibniz-Institut für Molekulare Pharmakologie (FMP), Campus Berlin-Buch, Robert-Roessle-Str. 10, 13125 Berlin, Germany

[5]State Key Laboratory of Bioactive Substance and Function of Natural Medicines, Institute of Materia Medica, Peking Union Medical College and Chinese Academy of Medical Sciences, 1 Xiannongtan Street, 100050 Beijing, China.

*Correspondence should be addressed to C.S. (schultz@embl.de) or M.N. (nazare@fmp-berlin.de)

Contents

Abbreviations

ACLT-pMx = anterior cruciate ligament transection and partial (~25%) meniscectomy
Boc = tert-butyloxycarbonyl
DIPEA = diisopropyl-ethyl amine
DMA = N,N-dimethylacetamide
DMF = dimethylformamide
DCM = dichloromethane
DMEM = Dulbecco's modified Eagle's medium
DOTA = 1,4,7,10-tetraazacyclododecane-1,4,7,10-tetraacetic acid
DOTAM = 1,4,7,10-tetraazacyclododecane-1,4,7,10-tetraacetic acid amide
DPBS = Dulbecco's Phosphate-Buffered Saline
ESI-MS = electrospray ionisation mass spectrometry
equiv. = equivalents
Fmoc = 9-fluorenylmethoxycarbonyl
Gd-DTPA = Gd-diethylene triamine pentaacetic acid
HFIP = 1,1,1,3,3,3-hexafluoro-2-propanol
HATU = 2-(7-Aza-1H-benzotriazole-1-yl)-1,1,3,3-tetramethyluronium hexafluorophosphate.
HPLC = high performance liquid chromatography
HRMS = high resolution mass spectrometry
LC-MS = liquid chromatography mass spectrometry
NMR = nuclear magnetic resonance
OA = Osteoarthritis
TFA = trifluoro-acetic acid

General methods

Unless otherwise noted, all reagents were purchased from commercial suppliers and used without further purification. All solvents used were of HPLC grade. Reactions were analyzed LC-MS. Reverse-phase HPLC was performed on a C18 column. LC-MS data were acquired using the Waters or HP-Agilent 1100 MSD system. NMR-data were recorded on a Bruker DRX-400 system in d_6-DMSO.

Synthesis of Contrast Agents

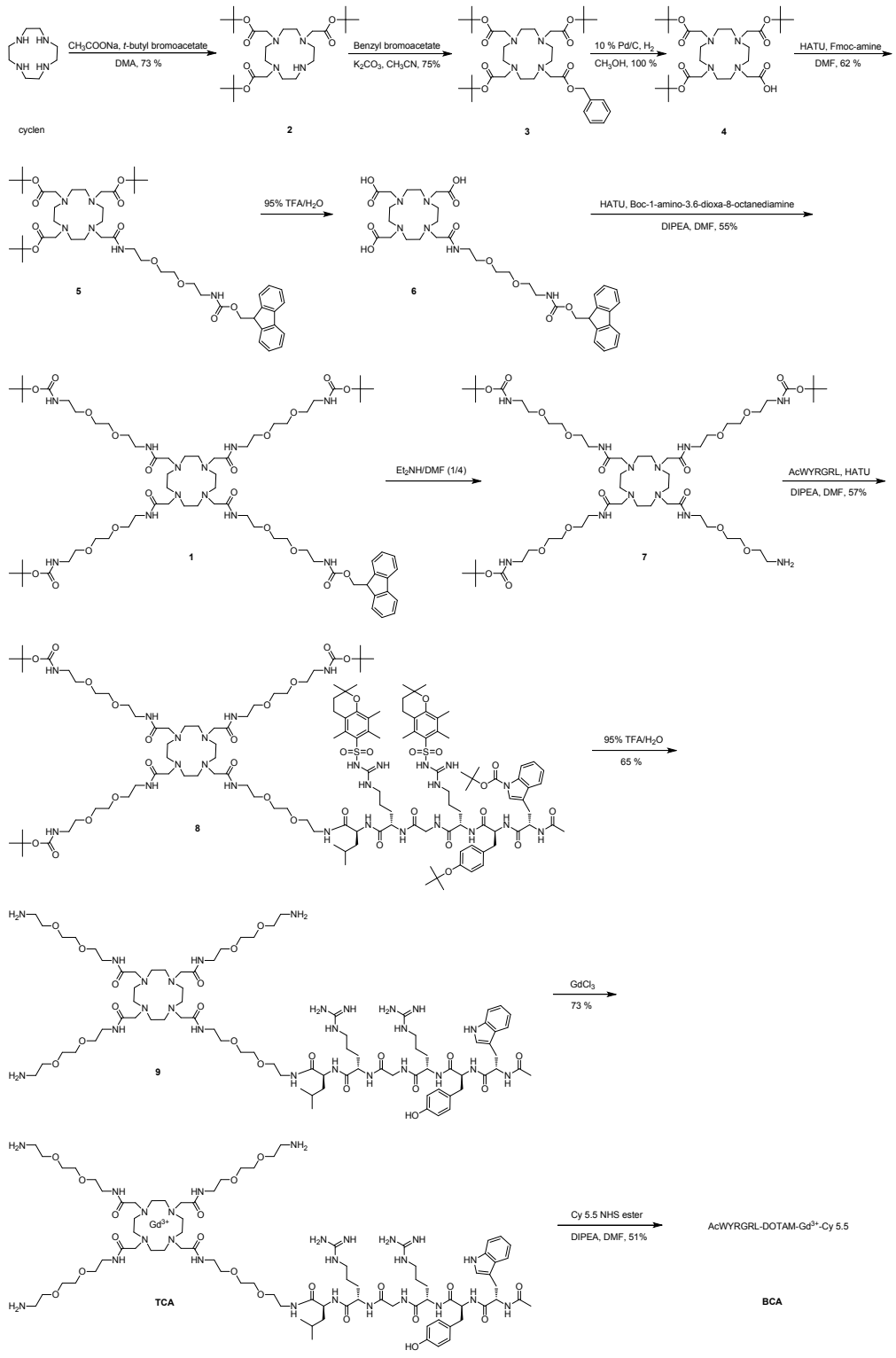

Scheme S1. Synthesis of cartilage targeting MRI contrast agent (**TCA**) and bimodal contrast agent (**BCA**).

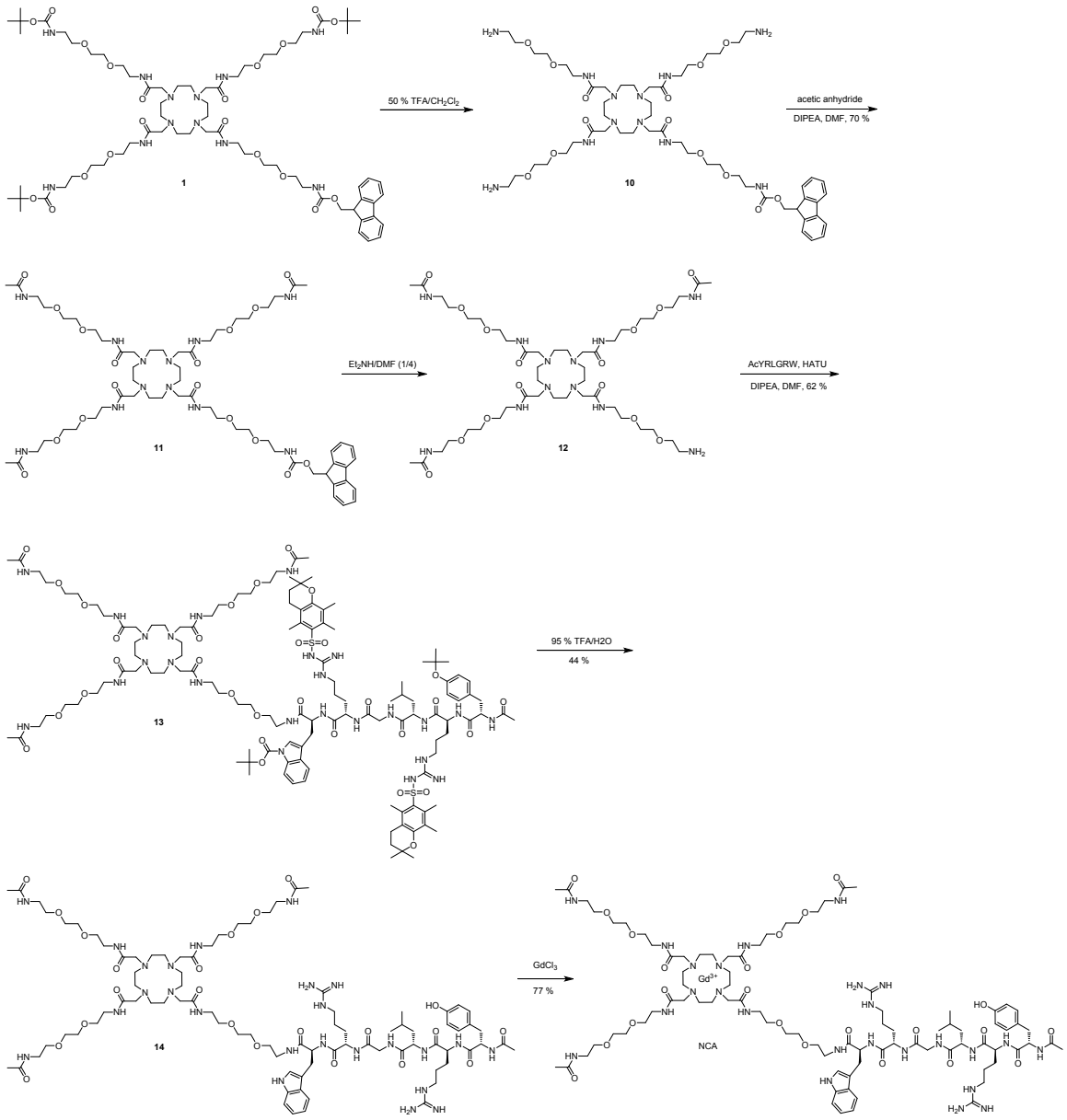

Scheme S2. Synthesis of non-targeting control MRI contrast agent (**NCA**).

General Procedures for Solid-Phase Peptide Synthesis

The peptides WYRGRL and YRLGRW were synthesized on solid resin using an automated peptide synthesizer (CEM Microwave Peptide Synthesizer) with standard F-moc chemistry. Both of the peptides were acetylated at the N terminus with a large excess of acetic anhydride and DIPEA. The fully protected peptide was cleaved from the resin using 30% HFIP in DCM and characterized by LC-MS.

Compound **2**

To a suspension of cyclen (5.00 g, 29 mmol) and sodium acetate (7.86 g, 96 mmol) in DMA (60 mL) at -20 °C was added a solution of *t*-butyl bromoacetate (18.7 g, 14.1 mL, 96 mmol) in DMA (20 mL) dropwise over a period of 0.5 hour. The temperature was maintained at -20 °C during the addition, after which the reaction mixture was allowed to come to room temperature. After 24 hours of vigorous stirring, the reaction mixture was poured into water (300 mL) to give a clear solution. Solid $KHCO_3$ (15 g, 150 mmol) was added portion wise, and compound **2** precipitated as a white solid. The precipitate was collected by filtration and dissolved in $CHCl_3$ (250 mL). The solution was washed with water (100 mL), dried ($MgSO_4$), filtered and concentrated to about 20-30 mL. Ether (250 mL) was added, after which compound **2** crystallized as a white fluffy solid. Yield: 12.5 g (73 %). ESI-MS found: $[M+H]^+ = 515.5$.[1]

Compound **3**

To a suspension of compound **2** (12.5 g, 24 mmol) in acetonitrile, K_2CO_3 powder (5.0 g, 36 mmol, 1.5 eq.) and subsequently benzyl bromoacetate (5.6 g, 28.8 mmol, 1.2 eq.) were added. Reaction was stirred at room temperature for 3 hours. Reaction process was monitored by TLC ($CHCl_3$-EtOH (9:1), compound **3**: *Rf* = 0.8). The precipitated solids were removed by filtration and the filtrate was concentrated to give the crude product, which was purified by silica gel column chromatography using CH_2Cl_2-MeOH (100:0 → 90:10) to give colorless solids compound **3** (Yield: 12.0 g, 75 %). ESI-MS found: $[M+H]^+ = 663.5$.[2]

Compound **4**

Compound **3** (1.2 g, 18 mmol) was hydrogenolyzed over 10 % Pd on carbon (180 mg) in MeOH (100 mL) for 12 h under an ambient pressure of hydrogen. The Pd/C was removed by filtration and the MeOH removed by evaporation. Compound **4** was analyzed by LC-MS and used without further purification. ESI-MS found: $[M+H]^+ = 573.4$.[2]

Compound **5**

1 equiv. compound **4** (572 mg, 1 mmol), 1 equiv. HATU (380 mg, 1 mmol) and 4 equiv. DIPEA (0.7 ml, 4 mmol) were dissolved in 10 ml DMF. After 10 min, 1 equiv. 1-(9-

Fluorenylmethyloxycarbonyl-amino)-3, 6-dioxa-8-octaneamine hydrochloride (407 mg, 1 mmol) was added to the reaction mixture and stirred 10 min. under argon at room temperature. The solution was diluted with EtOAc (50 mL), and washed with water 2×50 mL. The organic layer was dried over $MgSO_4$. Removal of the volatiles in vacuo provided pale yellow oil, which was purified by silica gel chromatography with MeOH–CH_2Cl_2 (0-10%). Yield: 570 mg, 62 %, . ^{1}H NMR (d_6-DMSO, 400MHz): δ 8.20 (t, J = 4.8 Hz, 1H, -N*H*), 7.89 (d, J = 7.6 Hz, 2H, -Ar), 7.68 (d, J = 7.6 Hz, 2H, -Ar), 7.41 (t, J = 6.8 Hz, 2H, -Ar), 7.32 (t, J = 6.8 Hz, 2H, -Ar), 7.29 (t, J = 5.7 Hz, 1H, -N*H*), 4.29 (d, J = 6.8 Hz, 2H, -CH_2O-), 4.20 (t, J = 6.8 Hz, 1H, -C*H*Ar-), 3.51-2.49 (m, 36H, -CH_2-), 1.43-1.41 (m, 27H, -CH_3). ^{13}C NMR (d_6-DMSO, 100MHz): δ 172.5, 171.6, 162.3, 143.9, 140.7, 127.6, 127.0, 125.1, 120.1, 81.1, 80.9, 69.4, 68.9, 40.2, 38.9, 38.2, 35.8, 30.8, 27.8, 27.6. ESI-MS calcd. for $C_{49}H_{76}N_6O_{11}$: 925.2; found: $[M+H]^+$ = 926.7.

Compound **6**

For the removal of the *t*Bu-group, compound **5** (925 mg, 1 mmol) was dissolved in 10 ml 95% TFA/H_2O and the reaction mixture was stirred for 2 hours under argon at room temperature. The reaction was monitored by LC-MS. After the reaction was complete, the solvent was 3 times co-evaporated with toluene. The crude product was used without further purification in the next step. ESI-MS calcd. for $C_{37}H_{52}N_6O_{11}$: 756.9; found: $[M+H]^+$ = 758.4.

Compound **1**

1 equiv. compound **6** (1 mmol), 3 equiv. HATU (1140 mg, 3 mmol) and 12 equiv. DIPEA (2100 µL, 12 mmol) were dissolved in 30 ml DMF. After 10 min, 3 equiv. Boc-1-amino-3.6-dioxa-8-octanediamine (745 mg, 3 mmol) was added to the reaction mixture and stirred 30 min. under argon at room temperature. The reaction was monitored by LC-MS. After the reaction was complete, the reaction solution was directly purified by HPLC to give compound **1** (800 mg, yield: 55 %) as a white powder. ^{1}H NMR (d_6-DMSO, 400MHz): δ 8.34 (bs, 3H, -N*H*), 7.94 (bs, 1H, -N*H*), 7.89 (d, J = 7.6 Hz, 2H, -Ar), 7.68 (d, J = 7.6 Hz, 2H, -Ar), 7.42 (t, J = 6.8 Hz, 2H, -Ar), 7.32 (t, J = 6.8 Hz, 2H, -Ar), 7.29 (t, J = 5.1 Hz, 1H, -N*H*), 6.74 (t, J = 4.78 Hz, 3H, -N*H*), 4.29 (d, J = 6.8 Hz, 2H, -CH_2O-), 4.21 (t, J = 6.8 Hz, 1H, -C*H*Ar-), 3.62-3.04 (m, 72H, -CH_2-), 1.37 (bs, 27H, -CH_3). ^{13}C

NMR (d_6-DMSO, 100MHz): δ 158.12, 158.10, 157.82, 158.78, 156.1, 155.6, 143.9, 140.7, 127.6, 127.0, 125.1, 120.9, 118.0, 115.1 77.6, 69.52, 69.47, 69.4, 69.2, 69.1, 68.8, 65.3, 54.5, 49.6, 46.7, 40.2, 40.0, 38.9, 28.2. ESI-MS calcd. for $C_{70}H_{118}N_{12}O_{20}$: 1447.79; found: $[M+2H]^{2+}$ = 724.6.

Compound **7**

For the removal of the Fmoc-group compound **1** (724 mg, 0.5 mmol) was dissolved in 2 ml Et_2NH/DMF (1/4) and the reaction mixture was stirred for 30 min. at room temperature. The reaction was monitored by LC-MS. After the reaction was complete, the solvent was removed under reduced pressure. The crude product was used without further purification in the next step. ESI-MS calcd. for $C_{55}H_{108}N_{12}O_{18}$: 1225.5; found: $[M+2H]^{2+}$ = 613.5

Compound **8**

1 equiv. AcWYRGRL (295 mg, 0.25 mmol), 1 equiv. HATU (95 mg, 0.25 mmol) and 4 equiv. 2,4,6-collidine (132 µl, 1 mmol) were dissolved in 20 ml DMF. After 10 min, 1 equiv. 1 equiv. compound **7** (306 mg, 0.25 mmol) was added to the reaction mixture and stirred 30 min. under argon at room temperature. The reaction solution was directly purified by HPLC to give compound **8** (400 mg, yield: 57 %) as a white powder. ESI-HRMS calcd. for $C_{134}H_{219}N_{25}O_{34}S_2$: 2786.56174; found: 2786.56164 ($[M+2H]^{2+}$ = 1394.28810).

Compound **9**

For the removal of all protecting groups, compound **8** was dissolved in 10 ml 95 % TFA/H_2O and the reaction mixture was stirred for 3 hours under argon at room temperature. The reaction was monitored by LC-MS. After the reaction was complete, the solution was co-evaporated 3 times with toluene. The crude product was purified by HPLC to give compound **9** (yield: 65 %) as a white powder. HRMS calcd. for $C_{82}H_{143}N_{25}O_{20}$: 1798.09412; found: 1798.09428 ($[M+4H]^{4+}$ = 450.53085). ^{1}H NMR (d_6-DMSO, 500MHz): δ 10.85 (bs, 1H, -N*H*), 9.20 (s, 1H, -N*H*), 9.05 (s, 1H, -N*H*), 8.83 (s, 1H, -N*H*), 8.08-6.75 (m, 23H, -N*H*,-NH_2, -Ar), 4.48-4.24 (m, 12H, -O*H*, -C*H*-, -NH_2),

4.00-2,00 (m, 82H, -CH_2-), 1.78-1.27 (m, 16H, -CH_2-,-NH-, -CH_3, -CH(CH_3)$_2$), 0.86 (d, J = 5.0 Hz, 6H, -CH(CH_3)$_2$).

Compound **10**

For the removal of all Boc protecting groups, compound **1** was dissolved in 10 ml 50 % TFA/CH_2Cl_2 and the reaction mixture was stirred for 1 hour under argon at room temperature. The reaction was monitored by LC-MS. After the reaction was complete, the solvent was co-evaporated 3 times with toluene. The crude product was used without further purification in the next step. ESI-MS calcd. for $C_{55}H_{94}N_{12}O_{14}$: 1147.43; found: $[M+H]^+$ = 1148.9.

Compound **11**

1 equiv. compound **10** (0.1 mmol), 6 equiv. acetic anhydride (62 mg, 0.6 mmol) and 12 equiv. DIPEA (210 µl, 1.2 mmol) were dissolved in 10 ml DMF and stirred 30 min. under argon at room temperature. The reaction was monitored by LC-MS. After the reaction was complete, the reaction solution was directly purified by HPLC to give compound **11** (90 mg, yield: 70 %) as a white powder. ^{1}H NMR (d_6-DMSO, 400MHz): δ 8.32 (bs, 3H, -8.20, -NH), 7.90-7.85 (m, 6H, -Ar, -NH), 7.68 (d, J = 7.2 Hz, 2H, -Ar), 7.42 (t, J = 7.2 Hz, 2H, -Ar), 7.34-7.29 (m, 3H, -Ar, -NH), 4.29 (d, J = 7.0 Hz, 2H, -CH_2O-), 4.21 (t, J = 7.0 Hz, 1H, -CHAr-), 3.68-3.13 (m, 72H, -CH_2-), 1.80 (bs, 9H, -CH_3). ^{13}C NMR (d_6-DMSO, 100MHz): δ 169.4, 127.6, 127.0, 125.1, 120.1, 99.5, 69.6, 69.5, 69.1, 66.8, 38.7, 38.5, 22.6. ESI-MS calcd. for $C_{61}H_{100}N_{12}O_{17}$: 1273.5; found: $[M+H]^+$ = 1273.9.

Compound **12**

For the removal of the Fmoc-group, compound **11** (50 µmol) was dissolved in 2 ml Et_2NH/DMF (1/4) and the reaction mixture was stirred for 10 min. at room temperature. The solvent was removed under reduced pressure. The crude product compound **12** was used without further purification in the next step. ESI-MS calcd. for $C_{46}H_{90}N_{12}O_{15}$: 1051.3; found: $[M+2H]^{2+}$ = 526.6.

Compound **13**

1 equiv. scrambled peptide sequence AcYRLGRW (79 mg, 50 µmol), 1 equiv. HATU (19 mg, 50 µmol) and 3 equiv. DIPEA (26 µl, 150 µmol) were solved in 2 ml DMF and stirred for 10 min. at room temperature. Subsequently, 1 equiv. compound **12** was added to the reaction mixture, which was stirred under argon at room temperature for 1 h. The reaction was monitored by LC-MS. After the reaction was complete, the reaction solution was directly purified by HPLC to give compound **13** (81 mg, yield: 62 %) as a white powder. HRMS calcd. for $C_{125}H_{201}N_{25}O_{31}S_2$: 2612.43616; found: 2612.43666 ($[M+2H]^{2+}$ = 1307.22561).

Compound **14**

For removal of all of the protecting groups, compound **13** (52 mg, 0.02 mmol) was dissolved in 2 ml 95 % TFA/H_2O and the reaction mixture was stirred for 3 hours under argon at room temperature (LC-MS monitoring). The solvent was 3 times co-evaporated with toluene, purified by HPLC to give compound **14** (17 mg, yield: 44 %) as a white powder. HRMS calcd. for $C_{88}H_{149}N_{25}O_{23}$: 1924.12581; found: 1924.12671 ($[M+3H]^{3+}$ = 642.38285). ^{1}H NMR (d_6-DMSO, 500MHz): δ 10.82 (d, J = 3.3 Hz, 1H, -N*H*), 9.04 (bs, 2H, -N*H*), 8.68 (s, 1H, -N*H*), 8.23-6.67 (m, 26H, -N*H*,-NH_2, -Ar), 4.50-4.30 (m, 6H, -O*H*, -C*H*-), 3.79-2,07 (m, 82H, -CH_2-), 1.82-1.25 (m, 25H, -CH_2-,-N*H*-, -CH_3, -C*H*$(CH_3)_2$), 0.86 (d, J = 5.0 Hz, 6H, -CH(CH_3)$_2$).

Gadolinium Complex Formation:

Complexes were prepared by adding a 1mM $GdCl_3$ stock solution to a DOTA-peptide ligand solution, in stoichiometric amounts (1:1). The pH was adjusted to 6 using 1 N NaOH and stirred for 48 h. and then centrifuged to remove any precipitated $Gd(OH)_3$. The presence of free Gd^{3+} was evaluated by colorimetry using xylenol orange as an indicator.[3] Resultant peptide complexes were further purified by HPLC to remove free the ligand. The purified complex solution was lyophilized to give the pure gadolinium complex as a powder solid.

TCA

Yield: 73 %, HRMS calcd. for $C_{82}H_{143}N_{25}O_{20}Gd$: 1956.01656; found: 1956.01628 ($[M+H]^{4+}$ = 489.25589).

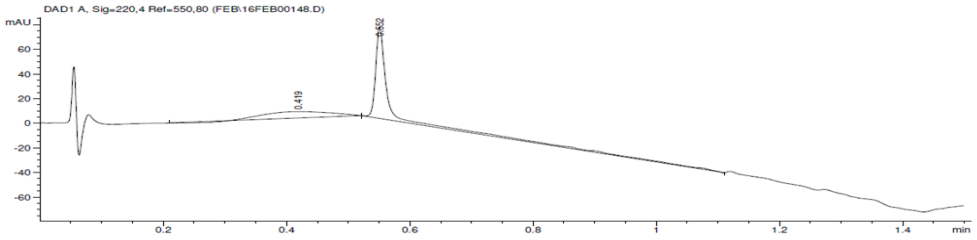

NCA

Yield: 77 %, ESI-MS calcd. for $C_{88}H_{149}N_{25}O_{23}Gd$: 2082.57; found: 2083.4 ($[M+H]^{4+}$ = 521.1).

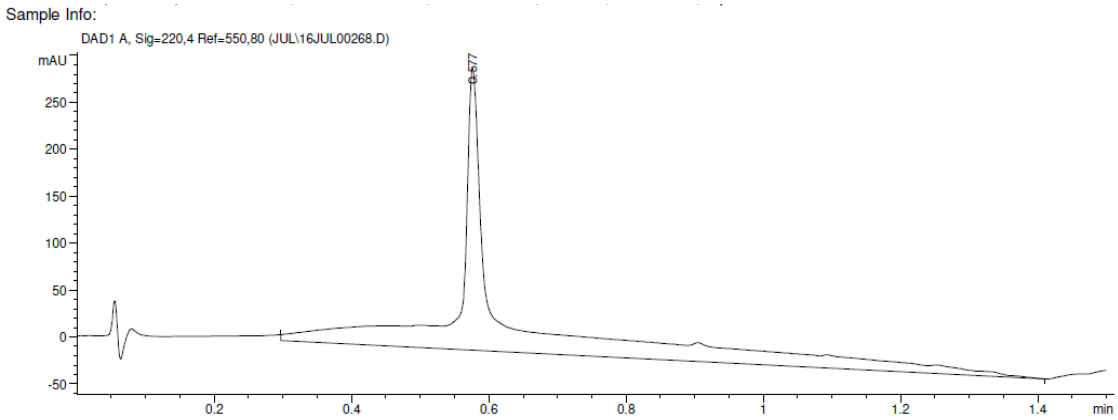

Bimodal cartilage-targeted imaging probes.

BCA

TCA (19 mg, 10 μmol) was dissolved in 1.5 ml DMF, followed by the addition of 1 equiv. Cy5.5 NHS ester (Succinimidyl Ester) (7 mg, 10 μmol) and 5 equiv. DIPEA (10 μl, 50 μmol). The reaction mixture was stirred under argon at room temperature for 12 hours. After the reaction was complete, the reaction solution was directly purified by HPLC to give to give **BCA** (13 mg, Yield 51 %) as a blue powder. HRMS calcd. for $C_{122}H_{184}N_{28}O_{20}Gd$: 2521.33792; found: 2521.33802 ($[M+H]^{4+}$ = 504.46906).

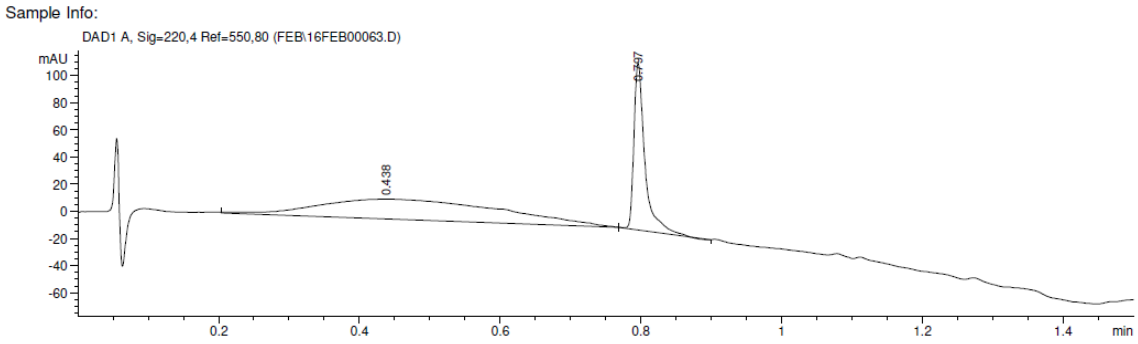

Histopathological scoring of joint damage in the rat ACLT-pMx OA model

Heterogeneity of disease progression in OA

The frequently used ACLT-pMx surgical OA model is a well validated model for development of localized osteoarthritis-like lesions in a relatively short time window. To compare the newly developed probe with the state-of-the art OA analysis in rat joints, we performed a longitudinal study on the disease progression. We assessed the severity of OA over a period of 12 weeks. Evaluation was performed by standard histology followed by a scoring method, as well as by characterization of the respective stage of the chondrophyte and pre-osteophyte formation.

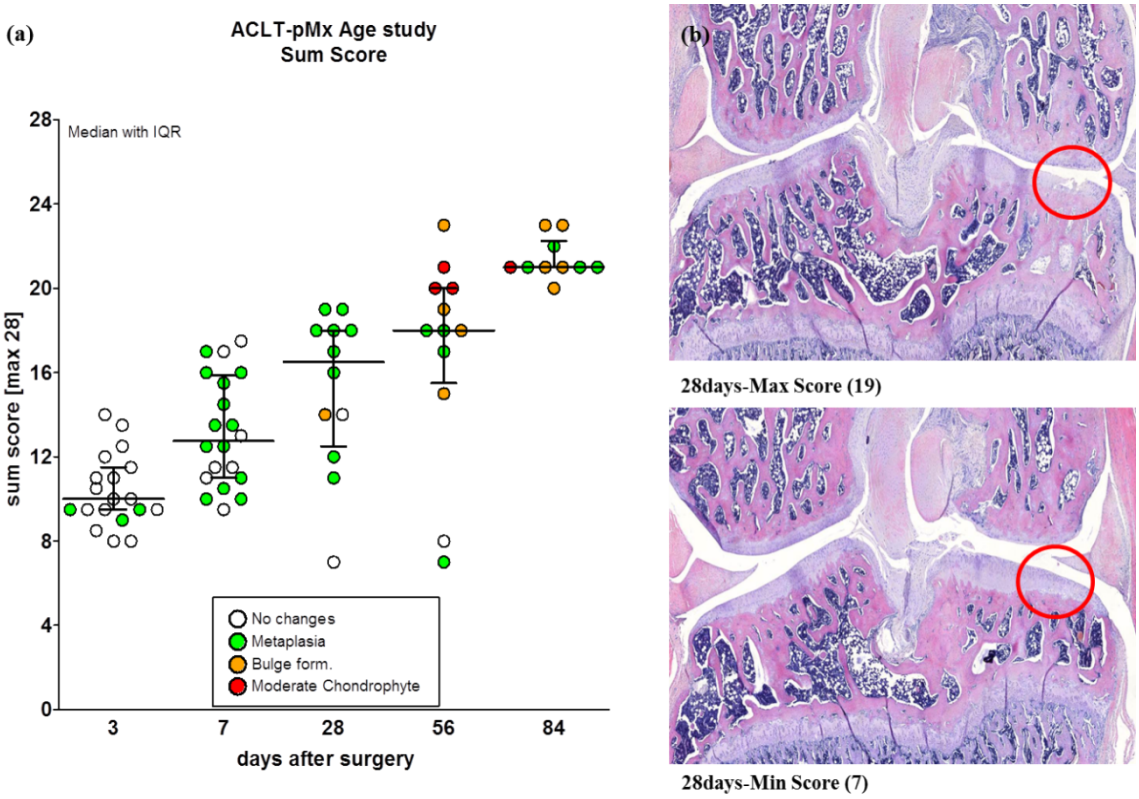

Figure S1. Data represents histopathological evaluations of joints from animals observed in a natural history of disease study after induction of OA by ACLT-pMx (n = 10-20, median with IQR). (a) Development of OA pathology over time; (b) Hematoxilin-Eosin-stained coronal section of a rat knee joint at day 28 post ACLT-pMx.

The rat ACLT-pMx model after 28 days post-surgery gave a median score of 16.5 (n = 12). However, as can be seen from disease progression data in Figure S1a (minimal score = 7, maximal score = 19) and Figure S1b, there is a significant variability in disease state and manifestation, resulting in the necessity of large numbers of animals required to obtain meaningful, statistical significant data in the pharmacological animal studies. Therefore, an imaging-based pre-selection of animals with a clearly defined disease phenotype by non-invasive *in vivo* imaging is reducing inter-animal variability and thereby allows improved observation of treatment effects by disease modifying OA drugs (DMOADs). An *in vivo* applicable imaging probe therefore has the potential to significantly reduce the number of animals required to be sacrificed.

Induction of osteoarthritis

Under deep isoflurane inhalation anesthesia, male skeletally mature Lewis rats (12 weeks of age, n = 10-20 animals/ group) were subjected to unilateral transection of the Anterior Cruciate Ligament plus partial (25%) removal of the anterior horn of the Medial Meniscus (ACLTpMx model).

Histopathological evaluation

At 3, 7, 28, 56 or 84 days after induction of OA by ACLT-pMX surgery coronal 7µm Hematoxylin-Eosin- and Safranin-O (SO)- stained paraffin sections were prepared throughout the joint and 5 slides with four consecutive histological sections per animal, showing the most severe pathology, were selected for evaluation.

Semiquantitative scoring

Sections were scored for the degree of joint damage in the four joint quadrants (medial Tibia and Femur, lateral Tibia and Femur, by two observers in a “blinded” fashion. To determine the degree of joint damage a modified 5-step Mankin-score (0-4), consisting of 7 sub-scores was used, (loss of chondrocytes in the superficial, intermediate and deep cartilage zones; cartilage fibrillations and fissures; cartilage ulceration; loss of proteoglycan staining; synovitis and subchondral bone sclerosis) resulting in a maximal

sum score of 28. The degree of OA joint damage was then determined by scoring the following parameters:

1. Chondrocyte changes (in the superficial cartilage zone)	Score
• normal	0
• swelling of chondrocytes	1
• focal loss of chondrocytes	2
• loss of chondrocytes in some regions	3
• almost complete loss of chondrocytes	4

2. Fibrillation and/or fissures in cartilage

• normal	0
• Minor surface irregularities	1
• widespread fibrillation and/or 1 small fissure	2
• 2 small or 1 medium fissures	3
• 3 small, 2 medium, or 1 large fissures	4

3. Cartilage erosion

• normal	0
• erosions of the superficial zone	1
• erosions extending into intermediate zone	2
• erosions extending into deep zone	3
• exposure of bone	4

4. Loss of proteoglycan

• normal	0
• staining reduced in 1-25 % of joint area	1
• staining reduced in 26-50 % of joint area	2
• staining reduced in 51-90 % of joint area	3
• staining reduced in >90 % of joint area	4

5. Loss of chondrocytes in intermediate and deep zones of cartilage

• normal	0

- slight focal decrease 1
- moderate decrease in cells 2
- widespread decrease (≥ 50% of cartilage area) 3
- almost complete loss of cells 4

6. Synovial changes including synovitis

- normal 0
- plus/or increase in number of lining cells 1
- plus/or thickening of sub-synovial tissue 2
- plus/or infiltration of few inflammatory cells 3
- plus/or infiltration of many inflammatory cells 4

7. Sclerosis of subchondral bone

- normal 0
- beginning increase in thickness 1
- moderate increase 2
- marked increase 3
- no marrow space left in > half of the area 4

Maximal total sum score 28

Spin-lattice relaxivity (r_1) measurements of MRI contrast agents TCA, NCA, BCA and Gd-DTPA

The suitability of Gd-loaded contrast agents for MRI applications was evaluated by taking T_1 weighted images of DPBS solutions of Gd-DTPA, **TCA**, **NCA** and **BCA** with different concentrations up to 0.20 mM (per Gd^{3+} ion).

In order to obtain quantitative information about the efficiency of Gd-loaded compounds as MRI contrast agents, we determined their molar spin–lattice relaxivity (r_1) at 25°C, 7.0 T using inversion recovery method.[4]

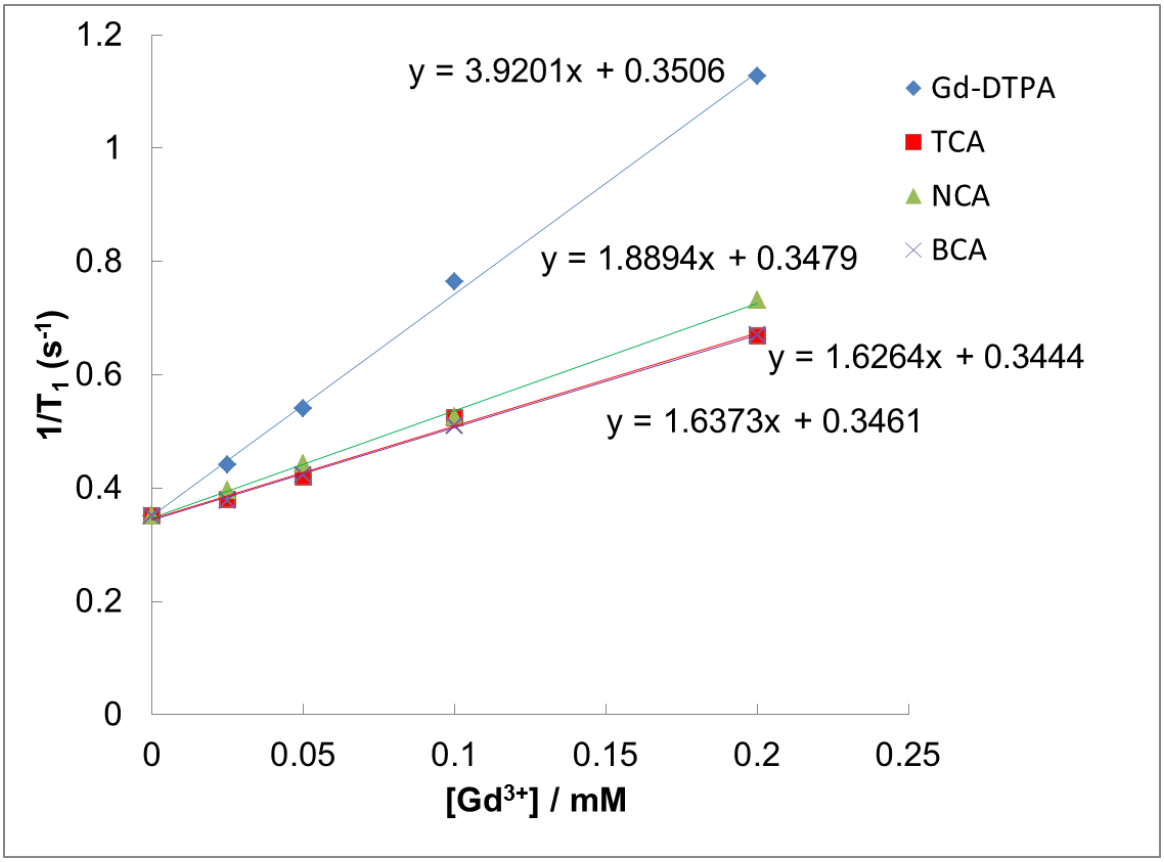

Figure S2. Spin-lattice relaxivity (r_1) of contrast agents **Gd-DTPA**, **TCA**, **NCA** and **BCA**.

Ex vivo MRI studies with pig cartilage explants

Whole-depth pig articular cartilage from knee joints of approx. 6 months old pigs was dissected into small discs of 4 mm in diameter. After dissection, the cartilage was allowed to rest for 17 h at 37 ºC under 5 % CO_2 in DMEM (Dulbecco's modified Eagle's medium) with 10 % (*v*/*v*) fetal bovine serum before being washed twice with DMEM without serum. Each cartilage piece was placed in one well of a round-bottomed 48-well plate with 1000 µl of DPBS with 0.2 mM of Gd-DTPA or **TCA**. After incubation at 37°C for 24 hours, the explanted pig cartilage pieces were washed 3 times for 10 min each with DPBS buffer at 37 ºC to remove free contrast agent, then imaged using MRI (7 T Bruker Biospec). Gd-DTPA showed no change of T_1 in the *ex vivo* pig cartilage compared with native pig cartilage.

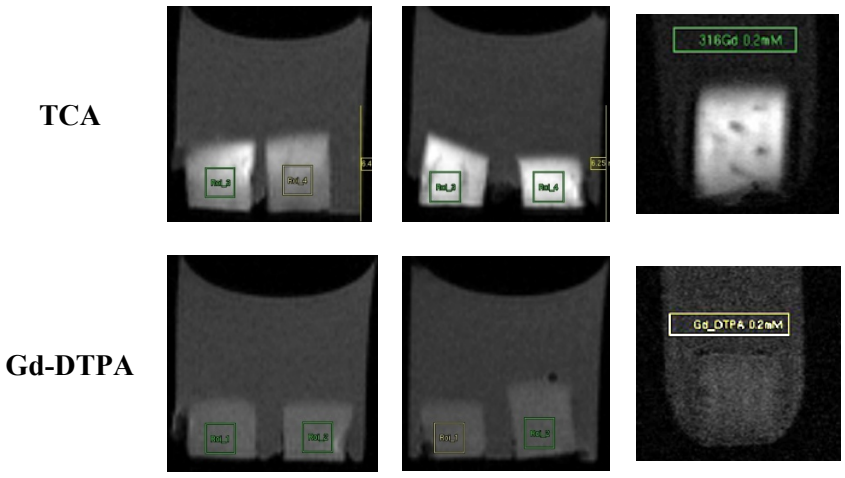

Figure S3. T_1-weighted MR Images of cartilage incubated with **TCA** (top) *vs* control Gd-DTPA (bottom) in 1 mL DPBS buffer (n = 5).

In vivo MRI studies with rats

MRI was performed using a 4.7 T Bruker BioSpec whole body MR imager. Male skeletally mature Lewis rats were anesthetized (by Isoflurane), fixed in supine position and both knees were placed within a transmitting/receiving wrist coil. Both knees were visualized simultaneously allowing the comparison of one knee with the other, in which the labeling characteristics of two different contrast agents **TCA** and **NCA** and their clearance from the knee joint were simultaneously monitored over time. Statistical analysis were performed with the software Prism (version 6.0, Graphpad Software, La Jolla, USA) using the students t-test.

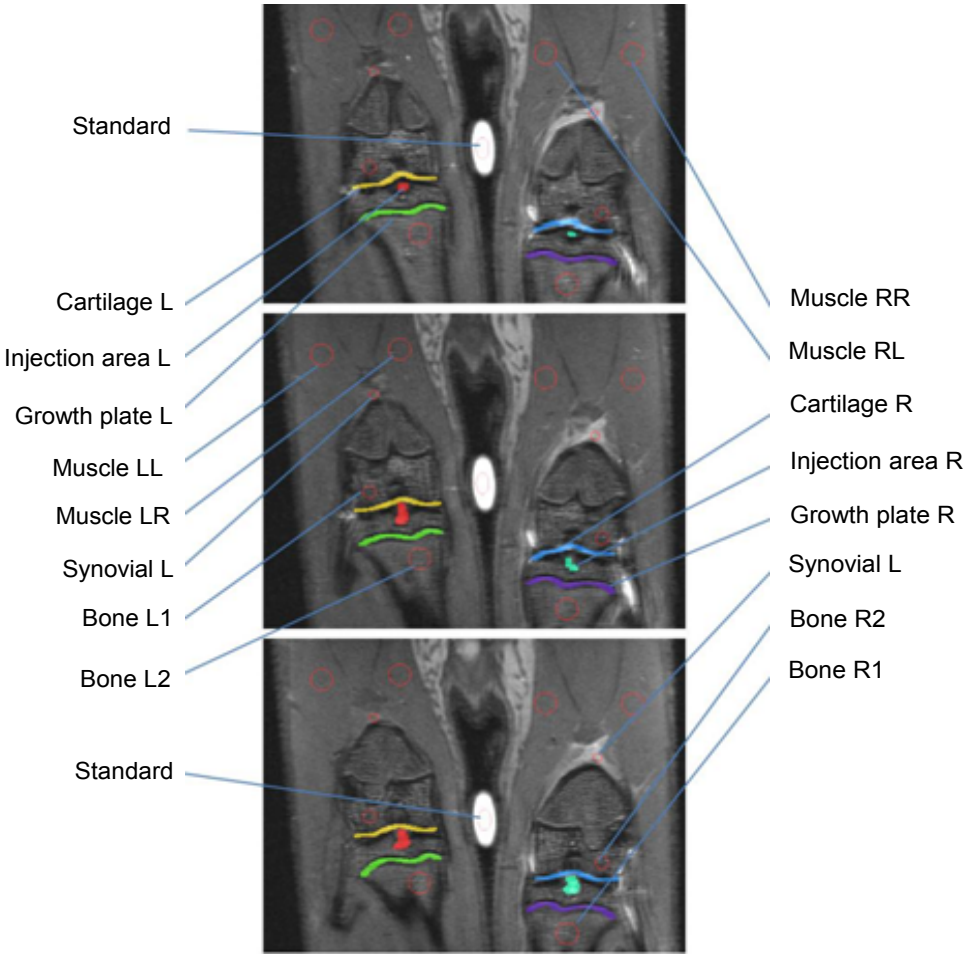

Figure S4. Definition of the femoral cartilage region, tibia growth plate region, injection area region, muscle regions, bone regions, synovial region and standard region in a T1-weighted image.

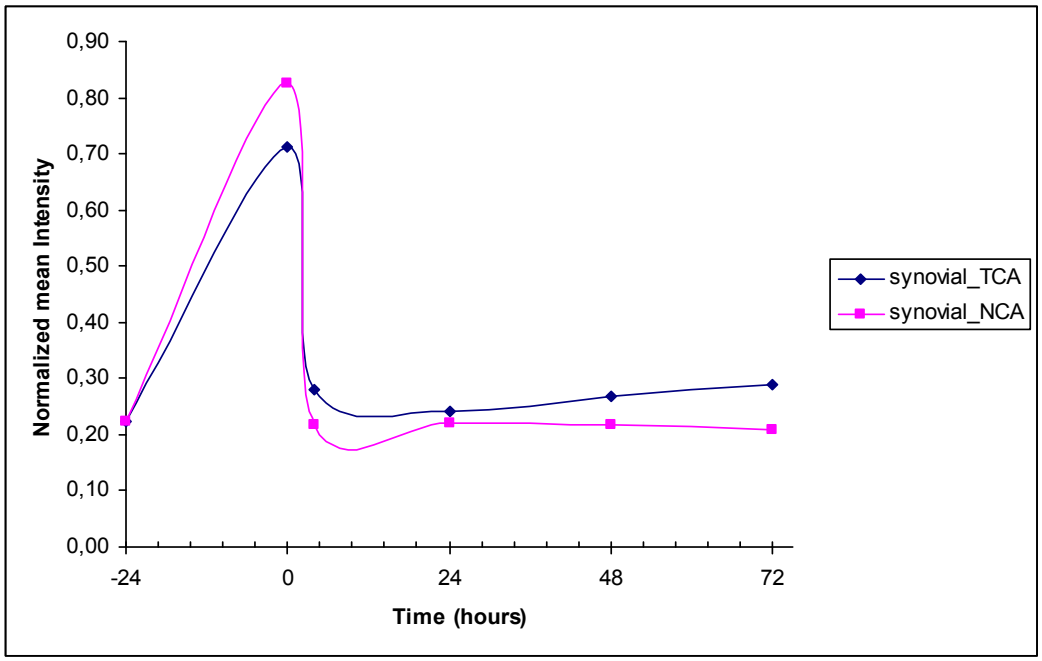

Figure S5. Plots of normalized mean intensities (n = 4) of the synovial areas before and after intra-articular injection of **TCA** and **NCA**.

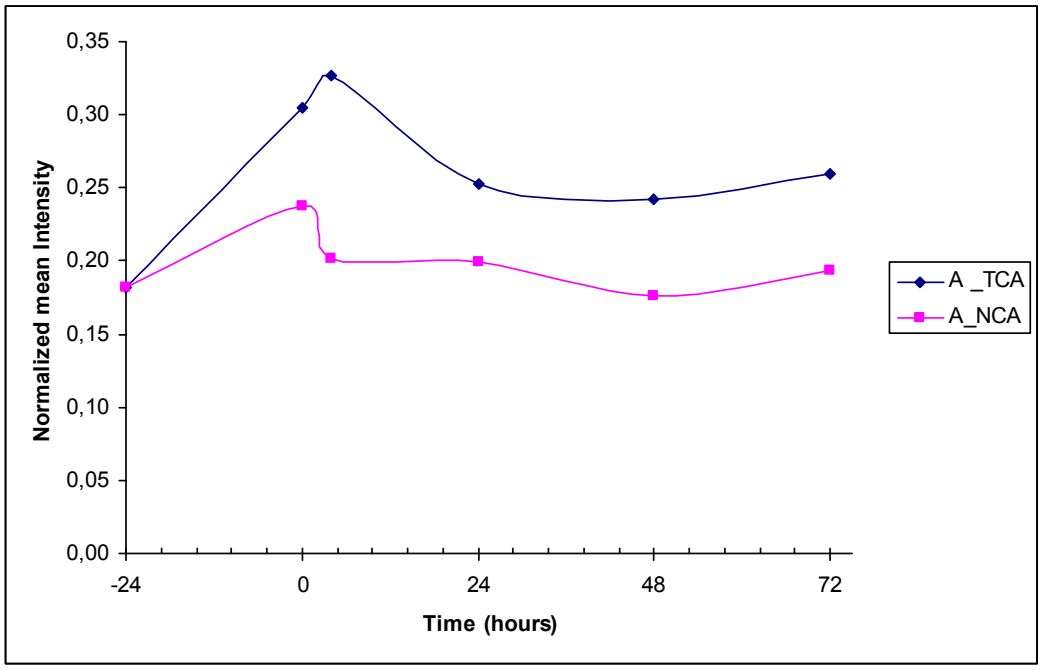

Figure S6. Plots of normalized mean intensities (n = 4) of the injection areas before and after intra-articular injection of **TCA** and **NCA**.

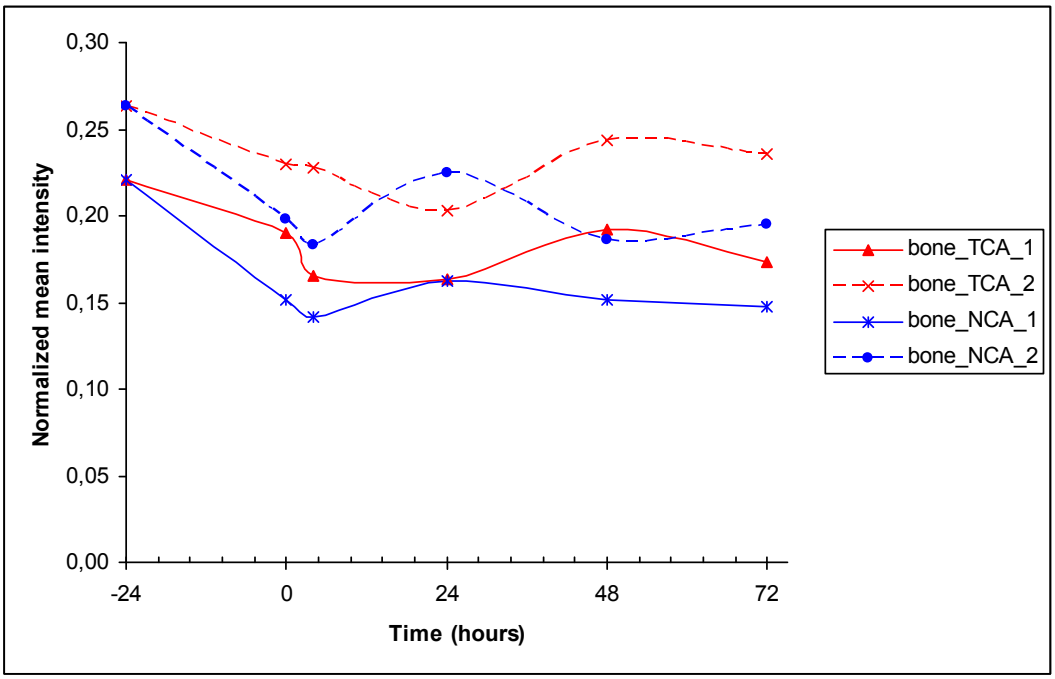

Figure S7. Plots of normalized mean intensities (n = 4) of the bone areas before and after intra-articular injection of **TCA** and **NCA**.

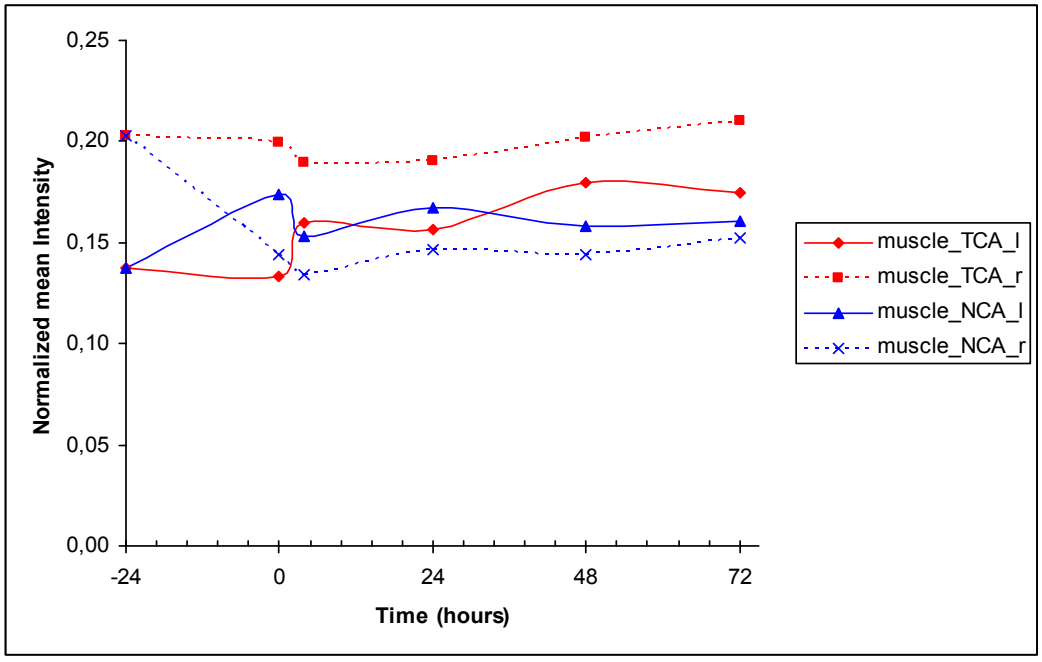

Figure S8. Plots of normalized mean intensities (n = 4) of the muscle areas before and after intra-articular injection of **TCA** and **NCA**.

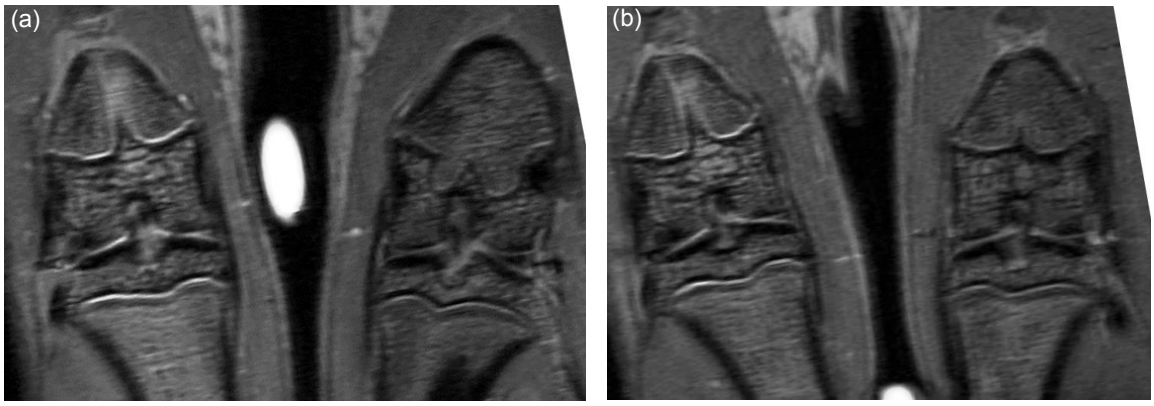

Figure S9. MR images of rat knees of contrast agents TCA (left) and NCA (right), (a) 48 hours after intra-articular injection, (b) 72 hours after intra-articular injection.

Near-infrared fluorescence (NIRF) signals were observed both in the matrix compartment and within chondrocytes. The pericellular matrix (more specifically the edges of pericellular matrix) and the cell nuclei were substantially free from signal.

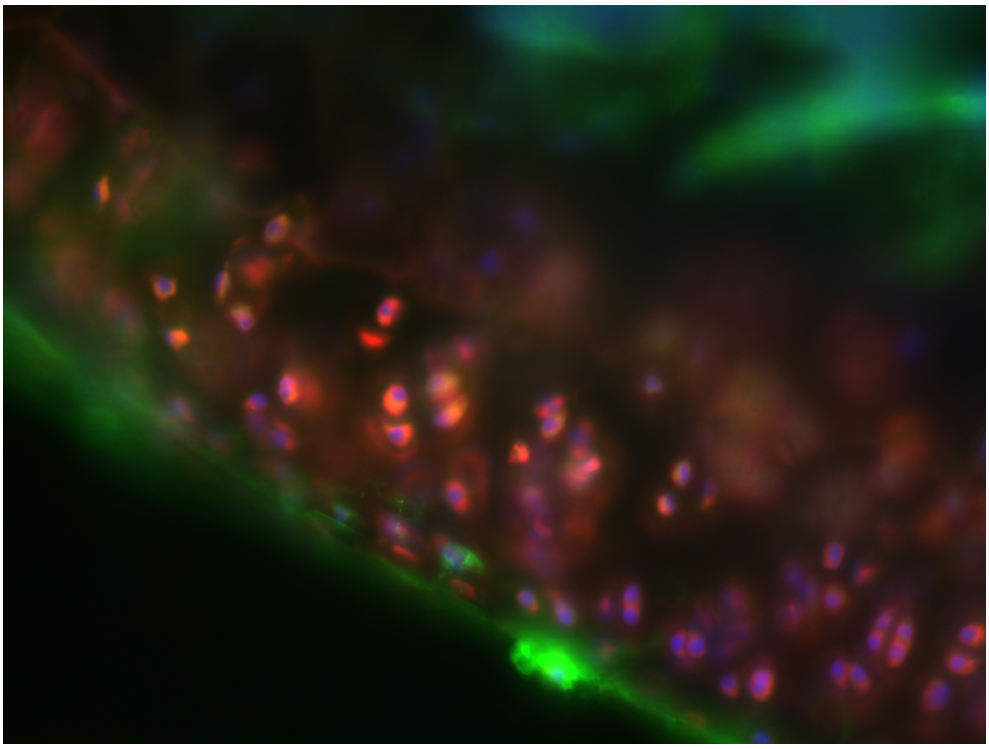

Figure S10. Merged image of probe distribution in articular cartilage of health knee joints at 48 hours after intra-articular injection. DAPI nuclear stain (blue), Perlecan stain (green), probe (red).

Immunofluorescence staining for type IIA procollagen

Type IIA procollagen IF staining was strong in the cells with stronger NIRF signals in the ACLT-pMx joint osteophyte regions.

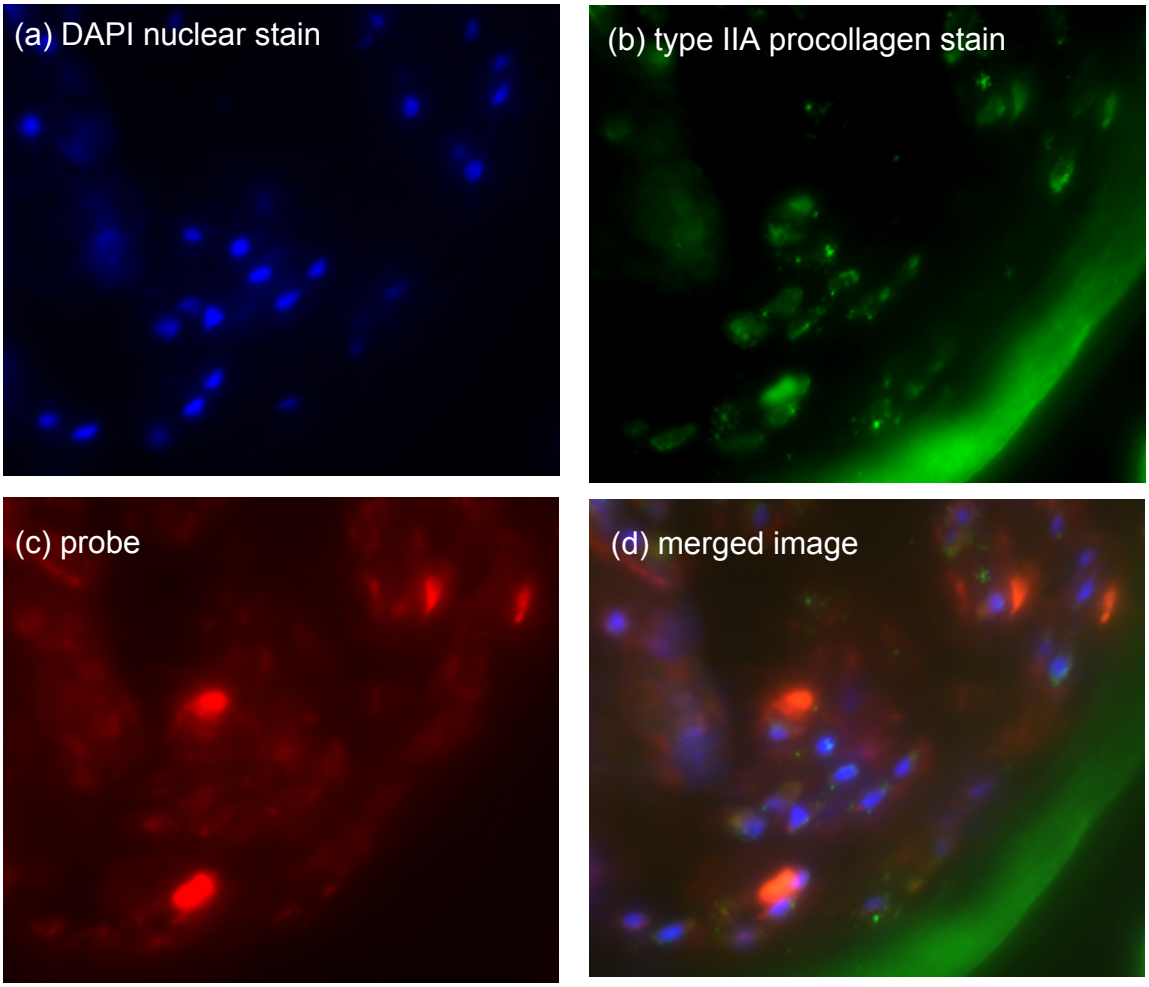

Figure S11. Fluorescent images of probe distribution in osteophyte areas in ACLT-pMMx rats at 48 hours after intra-articular injection. (a) DAPI nuclear stain (blue), (b) type IIA procollagen stain, (c) probe (red), (d) merged image.

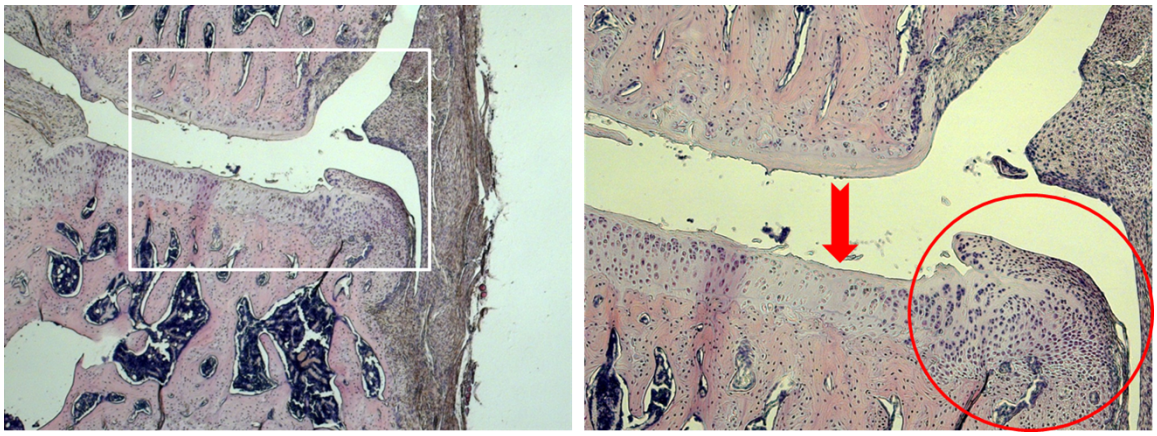

Figure S12. White frame in HE-stained overview (left hand side) in magnified view (right hand side): Note the incongruence of the medial femural condyle and the tibia plateau which potentially led to the metaplastic change (red circle) at the medial joint rim. This may have resulted in a less pronounced overall damage to the medial tibia plateau (red arrow) which is typically observed in this model at day 28 post ACLT-pMx surgery.

Histological studies of non-targeting control probe CP.

A control experiment was done with Cy 5.5 labelled DOTAM lacking the targeting peptide. This conjugate showed no cartilage targeting effect.

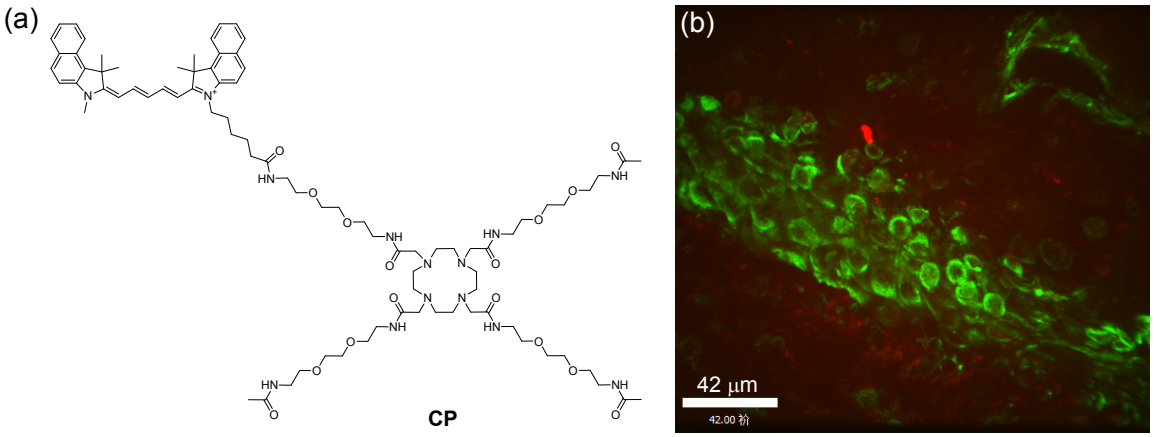

Figure 13S. Structure (a) and histological studies (b) of non-targeting control probe **CP**. Merged images of probe distribution (Cy5.5, red) with perlecan (Alexa-488, green) in articular cartilage 24 hours after intra-articular administration in mice knee joints.

References.

1. Jagadish, B., Brickert-Albrecht, G. L., Nichol, G. S., Mash, E. A., Raghunand, N. *Tetrahedron Lett.* **2011**, *52*, 2058-2061.
2. Strauch, R. C., Mastarone, D. J., Sukerkar, P. A., Song, Y, Ipsaro, J. J., Meade, T. J., *J. Am. Chem. Soc*. 2011, *133*, 16346-16349.
3. Geninatti Crich, S.; Lanzardo, S.; Barge, A.; Esposito, G.; Tei, L.; Forni, G.; Aime, S. *Mol. Imaging*, **2005**, *4*, 7-17.
4. Vold, R. L., Waugh, J. S., Klein, M. P., Phelps, D. E. *J. Chem. Phys.* **1968**, *48*, 3831-3832.